Structure, stability, and magnetism of Sc_nAl ($n=1-8,12$) clusters: Density-functional theory investigations

Fu-Yang Tian, Qun Jing, and Yuan-Xu Wang*
Institute of Computational Materials Science, School of Physics and Electronics, Henan University, Kaifeng 475004, People's Republic of China
(Received 27 August 2007; published 18 January 2008)

Equilibrium geometries and electronic and magnetic properties of small Sc_nAl ($n=1-8,12$) clusters have been studied based on the density-functional theory with all-electron spin-polarized generalized gradient approximation. The calculated results show that the Al atom remains on the surface for $n=1-8$, but at the center of the $Sc_{12}Al$ cluster with a variable icosahedral structure (C_{3v}). Doping of the Al atom enhances the stability of the scandium clusters. Maximum peaks are observed for clusters of $n=3,6$ on the size dependence of the second-order energy differences and fragmentation energies, implying that the two clusters possess relatively higher stability. This study also reveals that the Al atom is seen to induce significant changes in the magnetic property of the host cluster. Especially, the magnetic moment of the Sc_nAl cluster is quenched for $n=3$, 5, and 7, and the total magnetic moment of the $Sc_{12}Al$ cluster is only $7\mu_B$ (but $19\mu_B$ for Sc_{13}).

DOI: 10.1103/PhysRevA.77.013202 PACS number(s): 36.40.Cg, 31.10.+z, 31.15.E−, 36.40.Qv

I. INTRODUCTION

Clusters exhibit many interesting properties that are neither atomiclike nor extended solidlike. It is expected that materials assembled from finite-sized clusters may have special properties. Thus much attention has been paid to the study of atomic clusters from both theoretical and experimental sides during the last few years [1,2]. For transition metal (TM) clusters, due to their fundamental importance in theory study and potential applications in magnetic material and chemical catalysis, iron, cobalt, and nickel *et al.* clusters have been investigated extensively [3–12]. Most of these studies have been carried out on the homogeneous clusters.

It is well-known that the dilute impurities alter the electronic structure and geometry of the bulk system. A similar phenomenon is also observed in the impurity-doped clusters. Recently, some meaningful improvements have been achieved in the study of the properties of a mixed cluster of TM atoms. By anion photodetachment photoelectron spectroscopy, Pramann *et al.* confirmed the high stability of the $Co_{12}V$ cluster with a most plausible icosahedral structure and the V atom in the cage center [13]. The different gap between spin-up and spin-down electrons in the Ni_nB clusters indicates that it could be used in the spin-polarized transport systems [14]. Yin *et al.* found the magnetic enhancement of Co_NMn_M ($N\leqslant 60$ and $M\leqslant 20$) clusters, which is not dependent on the cluster size and composition [15]. As for theoretical predictions, some attempts have been done on the Cu-Co, Ni-Cu, Ti_nAl, and $AlPb_n$ clusters [16–19], and so on.

Such investigations provide a powerful tool to gain insights into the physical and chemical properties of the doped system on a microscopic scale as a function of size and distribution. In the present work, we choose the Al atom as impurity and study the atomic structures and electronic properties of the Al-doped Sc bimetallic clusters. To best of our knowledge, there is no theoretical work on this system.

The electronic configuration of an isolated Sc atom is simple ($3d^14s^2$), and the experiment shows that the magnetic moments of the scandium clusters change nonmonotonically with the cluster size [20], but bulk scandium is paramagnetic. Therefore the scandium clusters may serve as an ideal system to understand the interplay among size, geometry, electronic structure, and magnetism. Based on such an idea, recently, the structural and magnetic properties of small pure scandium clusters have been studied by Yuan *et al.* [21] and Wang [22], respectively. However, the lowest energy structure of Sc_9 and spin multiply of Sc_6, Sc_8 are not consistent with each other. In this work, we focus on the structural, electronic, and magnetic properties of the Sc_nAl clusters. Meanwhile, the pure scandium clusters are also studied for comparison. It is found that the total magnetic moment of the $Sc_{12}Al$ cluster is only $7\mu_B$, but that of the Sc_{13} cluster is $19\mu_B$. Interestingly, although the central Al atom provides an antidirection magnetic moment, the decrease of the magnetic moments of the $Sc_{12}Al$ cluster are mainly contributed from the Sc atoms on the surface of the icosahedron. It may be important in technological application for the creation of new adjustable magnetic nanostructured materials. In Sec. II, we describe briefly the computational method and parameters; Sec. III presents the results and discussions; and summary and conclusions are given in the last section.

II. COMPUTATIONAL DETAILS

The selection of distinct initial geometries is important to the reliability of the ground state structures obtained. As the cluster size increases, the number of the possible geometries increases dramatically. In this paper, the conformations of the pure Sc_{n+1} ($n=1-8,12$) clusters are obtained firstly by reference to the configurations in Refs. [21,22], then we consider the previously calculated results of the Al, Y, La, Ti, and Zr clusters [11,23–27]. The geometries with different symmetries are also optimized for each size. During the course of choosing initial structures of the Sc_nAl clusters, we

*Corresponding author. wangyx@henu.edu.cn

have considered possible isomeric structures by placing the Al atom on each possible site of the Sc_n cluster as well as by substituting one Sc atom by the Al atom from the Sc_{n+1} cluster. The Ti_nAl, Ni_nB, and $AlPb_n$ stable isomers are also considered as candidates [14,18,19]. For all isomers of each cluster, the local minima of the potential energy surface are guaranteed by the harmonic vibrational frequencies without imaginary mode. Further, different spin multiplicities of the low-lying energy isomers are considered. In case the total energy decreases with increasing spin multiplicity, we consider an increasingly higher spin state until the energy minimum with respect to spin multiplicity is reached.

All calculations were performed using the density functional theory (DFT) provided by the DMol^3 package [28]. The density functional is treated with the generalized gradient approximation (GGA) corrected-exchange potential of the BLYP (the Lee-Yang-Parr correlation functional) [29,30]. We have chosen a basis set composed of a double numerical atomic orbital augmented by a polarized function (DNP), all-electron symmetry-unrestricted calculations are performed. In general the most accurate results can be obtained by the DNP basis set, which is comparable to 6-31G** sets. In the geometry optimization, the convergence thresholds were set to 0.002 Hartree/Å for the forces, 0.005 Å for the displacement, and 10^{-5} Hartree for the energy change. Self-consistent field calculations were done with a convergence criterion of 10^{-6} Hartree on the total energy. For accurate evaluation of the charge density, we have chosen the octuple scheme for the multipolar fitting procedure. A 0.001 Hartree of smearing was applied to the orbital occupation. The charge density and the magnetic moments were evaluated via the Mulliken population analysis.

The accuracy of the current computational scheme has been tested by the calculation on the scandium dimer, trimer, and aluminum dimer. For Sc_2, the quintet state is energetically lowest among all spin multiplicity in this calculation, which is in accordance with the earlier DFT results [21,22,31–33] and the experimental ones [34,35]. It is more stable than the triplet and septet states by 0.02 and 1.01 eV, respectively. The bond length of the scandium dimer is obtained as 2.649 Å, which agrees well with other theoretical work [36–40], the computed binding energy of 1.596 eV and vibrational frequency of 229.9 cm^{-1} are well-reproduced in comparison with the experimentally measured values of 1.65 ± 0.22 eV and 239.9 cm^{-1} [32,33,38,40], respectively. For Sc_3, our calculated spin multiplicity, bond length, and vibration frequency (3, 2.85 Å, and 247.9 cm^{-1}) are in agreement with the theoretical values and compare favorably with the experimental ones (3, 2.83 Å, and 248 cm^{-1}) [34,35]. The computed bond length for Al_2 is 2.50 Å, which is well-consistent with the experimental data 2.47 Å [41] and 2.57 Å [42]. These indicate that our approach provides an efficient way to study small Sc_{n+1} and Sc_nAl clusters.

III. RESULTS AND DISCUSSIONS

In this section, we present the equilibrium structures, stability, and the magnetic property of the Sc_{n+1} and Sc_nAl ($n=1-8,12$) clusters.

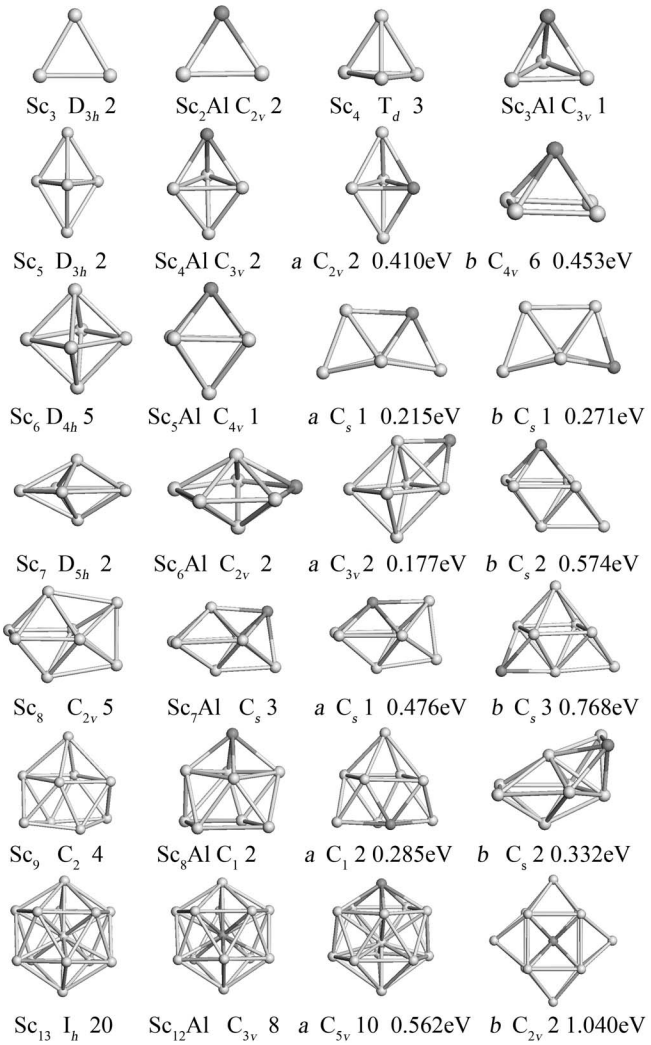

FIG. 1. Ground state structures of the Sc_{n+1} and Sc_nAl clusters, and two low-lying energy isomers (a,b) for doped clusters, their symmetry, multiplicity, and the energy difference compared to each of the ground state structures. The light and dark balls represent the Sc and Al atoms, respectively.

A. Structure of the Sc_{n+1} and Sc_nAl clusters

First, we discuss the evolutionary trend of the lowest-energy structures along with some typical low-lying energy configurations. For proper comparison, the equilibrium structures along with the host Sc_{n+1} geometries are shown in Fig. 1. Before beginning our discussion, we note that the ionic radius of the Al atom (0.721 Å for monovalent, 0.5 Å for trivalent) is smaller than that of the Sc atom (0.81 Å). Further, the binding energy per atom (E_b) of the ScAl dimer (1.010 eV/atom) is larger than that of the Sc_2 one (0.798 eV/atom), the bond lengths of the ScAl and Sc_2 dimers are 2.803 and 2.649 Å, respectively. Results for the scandium dimer and trimer have been discussed in Sec. II and are not repeated here.

For Sc_2Al and Sc_3Al, the lowest-energy structure of the Sc_2Al cluster turns out to be an isosceles triangle (C_{2v}), in which the Al atom is at the apex, the Sc-Sc distance (2.912 Å) is slightly longer than that of the Sc_2 dimer, and

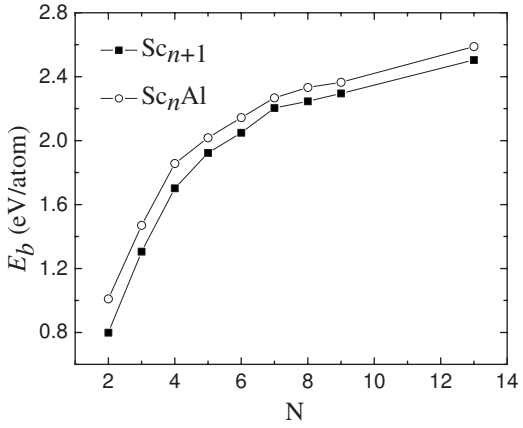

FIG. 2. The average binding energy per atom E_b of the Sc_nAl and Sc_{n+1} clusters.

the bond length of the Sc-Al is 2.686 Å. It is a spin doublet and lower by 0.183 eV in energy than the quartet state. The first three-dimensional (3D) structure occurs at $n=3$. Three Sc atoms form an equilateral triangle and the Al atom caps the surface resulting in a tetrahedral configuration (C_{3v}), and it is obtained as the ground state structure with spin singlet. One of the low-lying structures (C_s) is a spin triplet state with slightly higher energy (0.072 eV). While that of the Sc_4 cluster is a tetrahedron (T_d), which is the most compact structure. For the impurity-doped cluster, the early appearance of a 3D structure is not surprising.

Sc_4Al is a trigonal bipyramid which is similar to the Sc_5 configuration. The trigonal bipyramid but with two different substitution positions of the Al atom generates the lowest-energy structure of the Sc_4Al cluster with C_{3v} symmetry, and the low-lying energy structure with C_{2v} symmetry, in which the Al atom lies at the triangular ring. It is about 0.410 eV less stable. Another isomer with a higher energy (0.453 eV) is a square pyramid configuration where the four-coordinated Al atom is at its vertex position.

For $n=5$, the lowest-energy structure prefers the octahedron configuration with the Al atom at the vertex, it is a spin singlet, lower in 0.163 eV in energy than the triplet state. One low-lying configuration, above 0.215 eV in energy, is regarded as a capped triangle bipyramid on the base of the lowest-energy structure of the Sc_4Al cluster. The Al atom caps on the surface of the lowest-energy structure of the Sc_5 cluster resulting in another isomer configuration (C_{2v}), which is higher than the ground state structure of the Sc_5Al cluster by 0.271 eV. For the lowest-energy structure of the Sc_6 cluster, a quintet octahedron with D_{4h} symmetry is found to be energetically lower (0.06 eV) than the triplet state accordingly, which is the ground state structure reported [22]. This is well in agreement with the result reported in Ref. [21].

The lowest-energy structure of the Sc_6Al cluster is a distorted pentagonal bipyramid (D_{2h}) with an impurity Al atom becoming a part of the pentagonal ring, it is seen that the Al atom substitutes one Sc atom of the Sc_7 cluster. In addition, capped octahedron, tricapped tetrahedron, and bicapped square pyramid are considered. However, these isomers are higher in energy than the ground state structure, of which *a* and *b* are two low-lying structures with higher energy, 0.177 and 0.574 eV, respectively.

For Sc_8, the ground state structure is a quintet tetragonal antiprism and relaxes to an adjacent bicapped octahedron with C_{2v} symmetry, which agrees well with the result reported by Wang [22], it is energetically lower than the same structure with the spin triplet by 0.051 eV. It has been already reported that the configuration with the triplet state is predicted as the lowest-energy structure in Ref. [21]. With the Al atom substituting one Sc atom of the Sc_8 cluster, the lowest-energy structure (in Fig. 1) is obtained for the Sc_7Al cluster with C_s symmetry. The spin triplet is nearly degenerate with the single state, with the energy difference of 0.014 eV. The substitution for a bicapped octahedron but with a different substituting position of the Sc atom is well above the lowest-energy configuration (0.476 eV for configuration *a* and 0.768 eV for configuration *b*, respectively).

In case of the Sc_9 cluster, we found that the lowest-energy structure is a singly capped tetragonal prism (C_2) in a quartet state, and it is energetically lower than the bicapped pentagonal bipyramid in a doublet state by 0.188 eV, which is obtained as the ground state structure in Ref. [21]; and the similar singly capped tetragonal prism (C_s, but in a doublet state [22]) is energetically favored over the quartet state by 0.024 eV. As seen in Fig. 1, an Al atom capped on the distorted antiquadrangular prism of the Sc_8 cluster yields the lowest-energy structure for the Sc_8Al cluster. It is more stable than the tricapped trigonal prism by 0.285 eV. The structure of isomer (*b*) is above the lowest-energy structure by 0.332 eV, which is a bicapped pentagonal bipyramid with C_1 symmetry.

It is clear that the Al atom has tended to become a part of the clusters and can be looked upon as a substitutional impurity in the pure Sc_{n+1} clusters. The overall evolutionary trend shows that the ground state structures of the Sc_nAl clusters are similar to those of the Sc_{n+1} ones. The single Al atom sitting on the surface hardly affects the shape of the host cluster.

As far as $n=12$, we have considered all different sites for an Al atom in the icosahedron, cuboctahedron, and decahedron. The $Sc_{12}Al$ structure with an Al atom at the center is more stable as compared to the vertex position (0.562 eV), and is lower (1.040 eV) than the cuboctahedron (C_{2v}) with the central Al atom.

It is noticed that the lowest-energy structures of the Sc_6, Sc_8, and Sc_9 clusters are different from the previous works [21,22]. It is interesting to discuss the origin of this difference. First, under the same software package (DMol), we select an all-electron BLYP/DNP method, which is different from the all-electron BPW (constructed by the Perdew and Wang correlation function with Becke's exchange function) with the DNP basis set method in Ref. [21] and DSPP/PBE (DFT-based realtivistic semi-core pseudopotential with the PBE (Perdew-Burke-Ernzerhof exchange correlation functional) with the DND (a double numerical basis set including d-polarization functions) basis set methods in Ref. [22]. The ground state structures of the Sc_9 cluster are in disagreement with each other in Refs. [21] (bicapped pentagonal bipyramid) and [22] (capped tetragonal prism). Second, their partly filled *d* shells typically result in a number of alternative low-

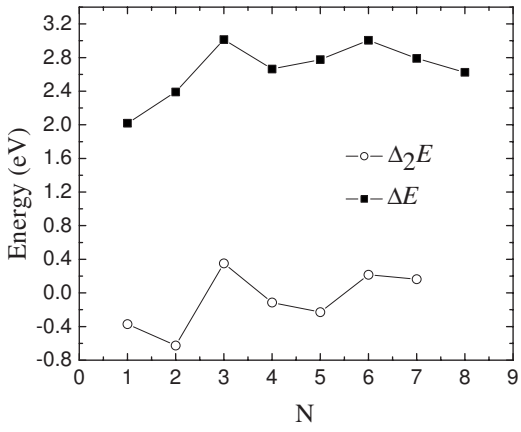

FIG. 3. The second-order energy difference $\Delta_2 E$ and fragmentation energy ΔE of the Sc_nAl ($n=1-8$) clusters.

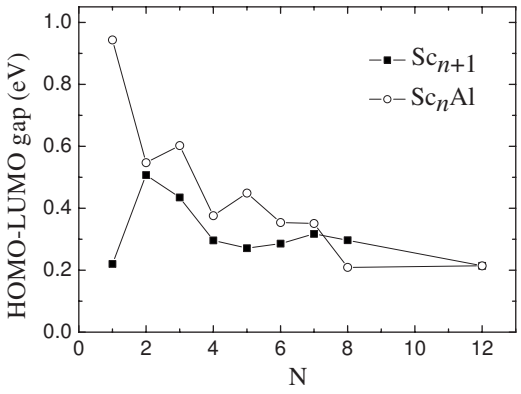

FIG. 4. The HOMO-LUMO gap of the Sc_nAl and Sc_{n+1} ($n=1-8,12$) clusters.

lying isomers within a very narrow energy range for transition metal clusters. For example, the energy difference of the different spin isomers is very small for the pure scandium clusters (such as Sc_6, Sc_8). Third, the occurrence of magnetism in clusters of nonmagnetic bulk scandium could bring additional difficulty to obtain the ground state structure.

B. Stability of the Sc_nAl clusters

In general the E_b increases sharply for very small clusters and then follows a plateau as the cluster size grows. Small humps or dips for the specific size of clusters signify their relative stability. The E_b of the Sc_nAl clusters (shown in Fig. 2) is calculated using the following equations: $E_b(Sc_nAl) = [nE(Sc) + E(Al) - E(Sc_nAl)]/(n+1)$, where $E(Sc)$, $E(Al)$, and $E(Sc_nAl)$ represent the energies of a Sc atom, an Al atom, and the total energy of the Sc_nAl cluster, respectively. For comparison, we also plot the E_b of the host Sc_{n+1} cluster in Fig. 2. As seen in this figure, the substitution of the Sc atom by an Al atom enhances the E_b of the host clusters. For Sc_nAl, the E_b evolves monotonically with total number of atoms in the cluster. Especially, for $n=2-4$, the E_b increases rapidly from 1.009 eV for the dimer to 1.856 eV for the tetramer which corresponds to the structure transition from two to three dimensions. The E_b increases gradually in the range $n=4-8$, in which the rate of increase becomes weak (only from 1.856 to 2.336 eV). The E_b of the Sc_nAl clusters shows a similar trend to that of the Sc_{n+1} clusters, in which the Sc_{13} cluster has an obvious peak value [21,22]. Thus we suggest that the E_b of the $Sc_{12}Al$ cluster is probably higher than its neighbor clusters. Generally speaking, the chemical bonding and the magnetic interaction could qualitatively explain the stability of the transition metal clusters. On the one hand, increasing the coordination and decreasing the interatomic distance could enhance the E_b of clusters; but both these factors tend to increase $3d$ electron delocalization, which could result in the reduction of the magnetic moments. On the other hand, the E_b could also be enhanced by increasing the exchange splitting of $3d$ orbit, which would increase magnetic moment. As result of the competition, the cluster

TABLE I. Symmetry S and total magnetic moment M (μ_B) for the Sc_{n+1} and Sc_nAl clusters; the magnetic moment M (μ_B) and the Mulliken charge Q (e) of the Al atom in the Sc_nAl clusters; and correlative properties of the partial low-lying structures.

	S	M		S	M	M (Al)	Q (Al)
Sc_2	$D_{\infty h}$	4	ScAl	$C_{\infty h}$	2	0.639	−0.046
Sc_3	D_{3h}	1	Sc_2Al	C_{2v}	1	0.178	−0.165
Sc_4	T_d	2	Sc_3Al	C_{3v}	0	0	−0.237
	T_d	4		C_s	2	0.045	−0.267
Sc_5	D_{3h}	1	Sc_4Al	C_{3v}	1	0.337	−0.346
Sc_6	D_{4h}	4	Sc_5Al	C_{4v}	0	0	−0.439
	C_{2h}	2		C_{4v}	2	−0.032	−0.412
Sc_7	D_{5h}	1	Sc_6Al	C_{2v}	1	0.005	−0.405
Sc_8	C_{2v}	4	Sc_7Al	C_s	0	0	−0.451
	C_{2v}	2		C_s	2	−0.053	−0.443
Sc_9	C_2	3	Sc_8Al	C_1	1	−0.011	−0.452
Sc_{13}	I_h	19	$Sc_{12}Al$	C_{3v}	7	−0.239	−0.334
	D_{3d}	15		C_{5v}	9	0.161	−0.499

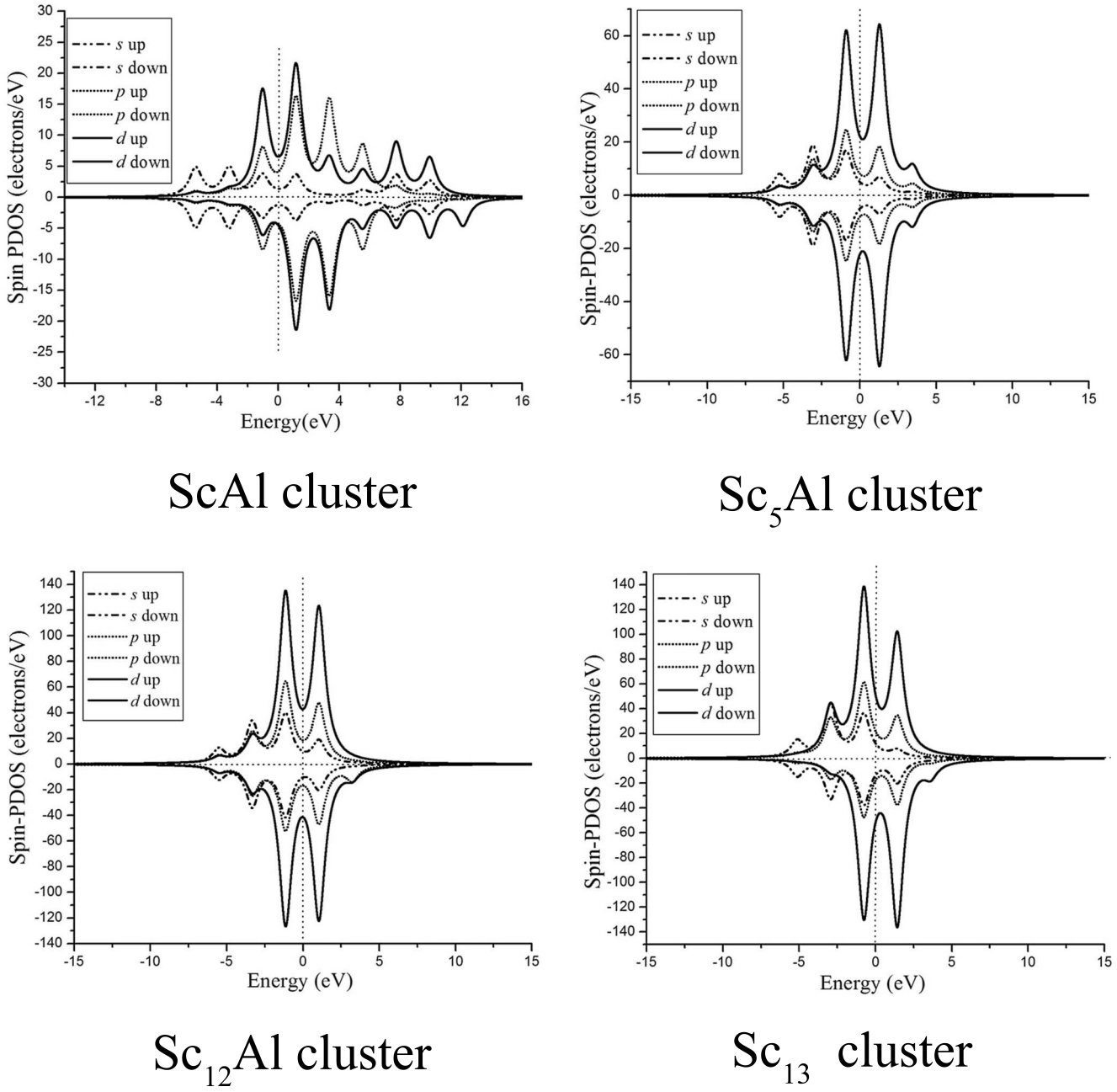

FIG. 5. The calculated SPDOS of the ScAl, Sc_5Al, $Sc_{12}Al$, and Sc_{13} clusters.

reaches its stable structure and magnetic state. From the following discussion, we would find that the magnetic moments of the Sc_nAl cluster are smaller than those of the Sc_{n+1} clusters.

In cluster physics, the second-order energy differences ($\Delta_2 E$) and fragmentation energy (ΔE) are sensitive quantities that reflect the relative stability of the investigated clusters. The $\Delta_2 E$ is often compared directly with the relative abundances determined in mass spectroscopy experiments. The ΔE shows the energy that one atom is separated from the host clusters. They are defined as the following formulas:

$$\Delta_2 E(\mathrm{Sc}_n) = E(\mathrm{Sc}_{n+1}\mathrm{Al}) + E(\mathrm{Sc}_{n-1}\mathrm{Al}) - 2E(\mathrm{Sc}_n\mathrm{Al}), \quad (1)$$

$$\Delta E = E(\mathrm{Sc}_{n-1}\mathrm{Al}) + E(\mathrm{Sc}) - E(\mathrm{Sc}_n\mathrm{Al}), \quad (2)$$

where $E(\mathrm{Sc}_n\mathrm{Al})$, $E(\mathrm{Sc}_{n+1}\mathrm{Al})$, $E(\mathrm{Sc}_{n-1}\mathrm{Al})$, and $E(\mathrm{Sc})$ represent the total energies of the most stable Sc_nAl, $Sc_{n+1}Al$, and $Sc_{n-1}Al$ clusters and a Sc atom, respectively. As shown in Fig. 3, particularly prominent maxima of $\Delta_2 E$ are found at $n=3,6$, indicating higher stability than their neighboring clusters. It is observed that, for the Sc_nAl clusters, the ΔE of the Sc_3Al (3.02 eV) and Sc_6Al (3.01 eV) clusters are higher than others clusters. Thus we can conclude that the magic clusters are found at $n=3,6$ for Sc_nAl.

The HOMO-LUMO gap (highest occupied-lowest unoccupied molecular orbital gap) is always considered to be an

TABLE II. Calculated spin up $Q\uparrow(e)$, spin down $Q\downarrow(e)$, total charge $Q(e)$ and net spin charge $Q\uparrow\downarrow(e)$ of the partial orbits for the Al (or Sc) atoms in the ScAl, $Sc_{12}Al$, and Sc_{13} clusters. ScAl (Al) and ScAl (Sc) means the Al and Sc atoms in the ScAl dimer, respectively. $Sc_{12}Al$ (Sc) and $Sc_{12}Al$ (Al) represent the Sc and Al atoms in the $Sc_{12}Al$ cluster, respectively, and the $Sc_{12}Al$ cluster has C_{3v} symmetry with the Al atom at the center. Sc_{13} (center) and Sc_{13} (outer) indicate the central and outer Sc atoms in the Sc_{13} cluster with the icosahedron structure, respectively.

Atom	Orbit	$Q\uparrow$	$Q\downarrow$	Q	$Q\uparrow\downarrow$
ScAl (Sc)	4*s*	0.706	0.747	1.453	−0.041
	4*p*	0.055	0.024	0.079	0.031
	3*d*	1.400	0.022	1.422	1.377
ScAl (Al)	3*s*	0.951	0.944	1.896	0.007
	3*p*	0.865	0.260	1.124	0.605
$Sc_{12}Al$ (Sc)	4*s*	0.515–0.532	0.567–0.596	1.082–1.122	−(0.052–0.070)
	4*p*	0.128–0.142	0.089–0.096	0.221–0.235	0.032–0.054
	3*d*	1.051–1.170	0.489–0.575	1.616–1.672	0.475–0.705
$Sc_{12}Al$ (Al)	3*s*	0.640	0.707	1.346	−0.067
	3*p*	0.799	0.975	1.774	−0.175
Sc_{13} (outer)	4*s*	0.596	0.465	1.060	0.131
	4*p*	0.172	0.066	0.239	0.106
	3*d*	1.496	0.200	1.696	1.295
Sc_{13} (center)	4*s*	0.390	0.391	0.781	0
	4*p*	0.205	0.032	0.237	0.173
	3*d*	1.115	0.902	2.017	0.231

important indicator of the electronic stability for small clusters. The magic clusters mostly have a very large HOMO-LUMO gap for the metal clusters. However, we do not find a strong correlation between the HOMO-LUMO gap and the energetic stability of the Sc_nAl clusters. The HOMO-LUMO gap of the Sc_{n+1} and Sc_nAl ($n=1-8$) clusters is shown in Fig. 4. Two prominent peaks appear at the Sc_3Al and Sc_5Al clusters, not the Sc_3Al or Sc_6Al clusters in Fig. 4. In general, the clusters with an odd number of electrons are not magic clusters. The high stability of the Sc_6Al cluster may stem from its highly symmetric close-packed geometry. It is well-known that the HOMO-LUMO gap is a characteristic quantity of metal clusters' electronic structure, and a system with a larger gap is less reactive. For $n=1-7$, the HOMO-LUMO gaps of the Sc_nAl clusters are larger than the corresponding Sc_{n+1} cluster but smaller for $n=8,12$. As the cluster size increases, the HOMO-LUMO gaps become smaller (from 0.950 to 0.213 eV), therefore these clusters should become more reactive and exhibit metal behavior as the cluster size increases.

C. Magnetic property of the Sc_{n+1} and Sc_nAl clusters

As mentioned in the Introduction, the most interesting property of scandium clusters is that bulk scandium is paramagnetic, but the experiment shows that the magnetic moments of the scandium clusters change nonmonotonically with the cluster size [20]. Thus it is valuable to study the magnetic property of the Sc_nAl clusters. Table I shows symmetry, calculated total magnetic moments of the ground state structures (Sc_{n+1},Sc_nAl), Mulliken charge, and magnetic moment of the Al atom in the Sc_nAl cluster. We find that total magnetic moments are $1\mu_B$ for Sc_3, Sc_5, and Sc_7, and $3\mu_B$ for Sc_9, but $4\mu_B$ for Sc_2, Sc_6, and Sc_8, and $2\mu_B$ for Sc_4, which are in general agreement with the previous work [21,22], except for the Sc_9 cluster. The magnetic moments for the even-numbered Sc_n clusters are relatively much larger than those neighboring odd-sized ones. From Table I it can be seen that doping of the Al atom decreases the magnetic moment of the host cluster. The magnetic moment of the Sc_nAl clusters is quenched for $n=3$, 5, and 7, in which the magnetic moment is $0\mu_B$ for the Al atom in the Sc_nAl clusters. However, the Sc_nAl clusters have total magnetic moments $1\mu_B$ for $n=2$, 4, 6, and 8, in which the magnetism may come from the odd number of valence electrons. It is interesting to note that the magnetic moment of the $Sc_{12}Al$ cluster ($7\mu_B$) is smaller than that of the Sc_{13} cluster ($19\mu_B$). As seen in Table I, the Al atom accepts charge from the Sc atoms, and the magnetic moment provided by the Al atom is very small, and even reverse, except for the ScAl and Sc_4Al clusters. For example, the magnetic moment of the Al atom decreases from $0.178\mu_B$ to $-0.239\mu_B$ for $n=2$, 4, 6, 8, and 12. For the vertex-site configuration (C_{5v}), the magnetic moment is $9\mu_B$, and the Al atom provides $0.161\mu_B$, and an accepted 0.499 Mulliken charge from the Sc atoms. The Sc atom at the center provides $0.234\mu_B$.

In order to further investigate the magnetic property, we show the spin up, spin down, and total charge for the partial orbital (4*s*, 4*p*, 3*d* for the Sc atom and 3*s*, 3*p*, for the Al atom) in Table II and spin partial density of state (SPDOS) in Fig. 5.

For the Sc_{13} cluster, the discrepancy of the magnetic moments between theory and experiment is very large, which

may be caused by the fact that the experimentally measured magnetic moment is an average value weighted according to the relative abundances of the isomers in the beam quantities that cannot be determined with high precision [21]. The Sc_{13} cluster (I_h) has the biggest magnetic moment of $19\mu_B$, but $15\mu_B$ for the Sc_{13} cluster with D_{3d} symmetry, which reflects that the total magnetic moments of the Sc_{13} clusters in terms of the above discussions depend on their geometries and spin states. The greatest magnetic moment of the Sc_{13} cluster may be related to its icosahedral structure because of increased symmetry-required degeneracy for electrons of different spins, which is similar to the Fe_{13} clusters reported by Dunlap [43]. Moreover, the magnetic effects of the different electrons in the incomplete $3d$ subshell do not cancel each other as they do in a completed subshell, giving rise to strong magnetism. From Table II, we find that $3d$ orbital charge plays a dominant role in the determination of the magnetism of the Sc_{13} cluster. The $4s$ and $4p$ orbits contribute only a small amount of net spin. As shown by the values of the spin up and spin down charge in Table II, the Sc atoms delocalize their $4s$ electrons, these delocalized-electrons mainly transfer to $3d$ orbit, and result in the enhancement of the magnetic moment. While the $Sc_{12}Al$ cluster (C_{3v}) has a small magnetic moment $7\mu_B$, it is the reason that the $4s$ orbit provides a reverse magnetic moment ($0.052\mu_B-0.069\mu_B$), and $3d$ orbit contributes a smaller magnetic moment ($0.475\mu_B-0.705\mu_B$, but $1.296\mu_B$ for Sc_{13}), which mainly cause the magnetic moment decrease, and the central Al atom provides a reverse magnetic moment. It can be seen in Table II that the magnetic moment of the central atom is smaller than that of surface atoms for the Sc_{13} and $Sc_{12}Al$ clusters. The magnetic interactions between the central and surface atoms are ferromagnetic for the Sc_{13} cluster, and antiferromagnetic for the $Sc_{12}Al$ cluster.

These magnetic properties are also proved by the SPDOS. The compared density is large for the $3d$ orbit. As seen in Fig. 5, there is a strong *spd* hybridization in the SPDOS for the ScAl, Sc_5Al, Sc_{13}, and $Sc_{12}Al$ clusters. For Sc_5Al, the spin up and down are very symmetric, indicating its zero magnetic moment. The Sc_{13} cluster shows strong asymmetric and maximal peak in the d orbit of the SPDOS, and the d orbit of every outer Sc atom provides 1.496 Mulliken charge for spin up, but only 0.200 for spin down as shown in Table II. Therefore the large magnetic moment of the Sc_{13} cluster is attributed to its asymmetric densities of d orbital states. For $Sc_{12}Al$, although the Mulliken charge distribution of the outer Sc atoms and relative intensity of the SPDOS are similar to those of the Sc_{13} cluster, its relatively symmetric spin up and spin down of the SPDOS results in its smaller magnetic moment than the Sc_{13} cluster.

IV. SUMMARY

The first-principles calculations were performed to study the structural, electronic, and magnetic properties of the Sc_nAl ($n=1-8,12$) clusters. The Sc_nAl clusters have similar geometries to the Sc_{n+1} ones, where the Al atom can be looked at as a substitutional impurity in the pure Sc_{n+1} clusters by a slight distortion. A systemic and detailed analysis of geometries, E_b, Δ_2E, and ΔE indicates that doping of the Al atom enhances the stability of the scandium clusters. The Sc_3Al and Sc_6Al clusters possess relatively higher stability for $n=1-8$. The HOMO-LUMO gap of the Sc_nAl clusters is larger than that of the Sc_{n+1} clusters for $n=1-7$, but, smaller for $n=8,12$. The Mulliken charge population and SPDOS of the Sc_nAl clusters show that doping of the Al atom reduces the magnetic moment of the host clusters and the magnetic moment of the Sc_nAl clusters is quenched around $n=3$, 5, and 7. The magnetic moment of the $Sc_{12}Al$ cluster is $7\mu_B$, which is much smaller than that of the Sc_{13} cluster ($19\mu_B$). Meanwhile, for the Sc_nAl clusters, the structural stability and magnetic moment appears to be the outcome of a delicate interplay among the cluster structure and *spd* hybridization between the Al and Sc atoms.

ACKNOWLEDGMENT

The authors are grateful to Dr. Guang-biao Zhang and Ling-ju Guo for helpful discussions.

[1] *Clusters and Nanostructured Materials*, edited by P. Jena and S. N. Behera (Nova Science, New York, 1996).
[2] J. A. Alonso, Chem. Rev. (Washington, D.C.) **100**, 637 (2000).
[3] S. Li, M. M. G. Alemany, and J. R. Chelikowsky, Phys. Rev. B **73**, 233404 (2006).
[4] V. Kumar and Y. Kawazoe, Phys. Rev. B **65**, 125403 (2002); **66**, 144413 (2002).
[5] A. N. Androtis, G. Mpourmoarkis, G. E. Froudakis, and M. Menon, J. Chem. Phys. **120**, 11901 (2004).
[6] J. P. Bucher, D. C. Douglass, and L. A. Bloomfield, Phys. Rev. Lett. **66**, 3052 (1991).
[7] H. M. Duan and Q. Q. Zheng, Phys. Lett. A **280**, 333 (2001).
[8] P. Bobadova-Parvanova, K. A. Jackson, S. Srinivas, and M. Horoi, J. Chem. Phys. **122**, 014310 (2005).
[9] T. Pawluk, Y. Hirata, and L. Wang, J. Phys. Chem. B **109**, 20817 (2005).
[10] J. L. Wang, G. H. Wang, and J. J. Zhao, Phys. Rev. B **66**, 035418 (2002).
[11] A. Lyalin, A. V. Solov'yov, and W. Greiner, Phys. Rev. A **74**, 043201 (2006).
[12] M. Kabir, A. Mookerjee, and D. G. Kanhere, Phys. Rev. B **73**, 224439 (2006).
[13] A. Pramann, K. Koyasu, and A. Nakajima, J. Phys. Chem. A **106**, 2483 (2002).
[14] M. Deshpande, D. G. Kanhere, and R. Pandey, Phys. Rev. A **71**, 063202 (2005).
[15] S. Yin, R. Moro, X. S. Xu, and W. A. de Heer, Phys. Rev. Lett. **98**, 113401 (2007).
[16] J. L. Wang, G. H. Wang, X. S. Chen, W. Lu, and J. J. Zhao, Phys. Rev. B **66**, 014419 (2002).

[17] P. A. Derosa, J. M. Seminario, and P. B. Balbuena, J. Phys. Chem. A **105**, 7917 (2001).
[18] J. Xiang, S. H. Wei, X. H. Yan, J. Q. You, and Y. L. Mao, J. Chem. Phys. **120**, 4251 (2004).
[19] D. L. Chen, W. Q. Tian, and C. C. Sun, Phys. Rev. A **75**, 013201 (2007).
[20] M. B. Knickelbein, Phys. Rev. B **71**, 184442 (2005).
[21] H. K. Yuan, H. Chen, A. S. Ahmed, and J. F. Zhang, Phys. Rev. B **74**, 144434 (2006).
[22] J. L. Wang, Phys. Rev. B **75**, 155422 (2007).
[23] F. C. Chuang, C. Z. Wang, and K. H. Ho, Phys. Rev. B **73**, 125431 (2006).
[24] H. K. Yuan, H. Chen, A. L. Kuang, A. S. Ahmed, and Z. H. Xiong, Phys. Rev. B **75**, 174412 (2007).
[25] C. C. Wang, R. N. Zhao, and J. G. Han, J. Chem. Phys. **124**, 194301 (2006).
[26] S. H. Wei, Z. Zeng, J. Q. You, X. H. Yan, and X. G. Gong, J. Chem. Phys. **113**, 11127 (2000).
[27] W. J. Zhao, X. L. Lei, Y. L. Yan, Z. Yang, and Y. H. Luo, Acta Phys. Sin. **56**, 5209 (2007).
[28] DMol is a density functional theory program distributed by Accelrys, Inc., 2006; B. Delley, J. Chem. Phys. **92**, 508 (1990); **113**, 7756 (2000).
[29] C. Lee, W. Yang, and R. G. Parr, Phys. Rev. B **37**, 785 (1988).
[30] A. D. Beche, J. Chem. Phys. **88**, 2547 (1988).
[31] H. Akeby, L. G. M. Pettersson, and P. E. M. Siegbahn, J. Chem. Phys. **97**, 1850 (1992).
[32] I. Papai and M. Castro, Chem. Phys. Lett. **267**, 551 (1997).
[33] A. Berces, Spectrochim. Acta, Part A **53**, 1257 (1997).
[34] L. B. Knight, R. J. Van Zee, and W. Weltner, Chem. Phys. Lett. **94**, 296 (1983).
[35] M. Moskovits, D. P. Dilella, and W. Limm, J. Chem. Phys. **80**, 626 (1984).
[36] S. Yanasigava, T. Tsuneda, and K. Hirao, J. Chem. Phys. **112**, 545 (2000).
[37] G. L. Gutsev, P. Jena, B. K. Rao, and S. N. Khanna, J. Chem. Phys. **114**, 10738 (2001).
[38] Z. J. Wu, H. J. Zhang, J. Meng, Z. W. Dai, B. Han, and P. C. Jin, J. Chem. Phys. **121**, 4699 (2004).
[39] C. J. Barden, J. C. Rienstra-Kiracofe, and H. F. Schaefer III, J. Chem. Phys. **113**, 690 (2000).
[40] K. A. Gingerich, Faraday Symp. Chem. Soc. **14**, 109 (1980).
[41] *Handbook of Chemistry and Physics*, 82nd ed., edited by D. R. Lide (CRC Press, New York, 2001).
[42] B. K. Rao and P. Jena, Appl. Phys. Lett. **57**, 2308 (1990); S. N. Khanna and P. Jena, Phys. Rev. Lett. **69**, 1664 (1992).
[43] B. I. Dunlap, Phys. Rev. A **41**, 5691 (1990); Z. Phys. D: At., Mol. Clusters **19**, 255 (1991).